NASA Contractor Report 4087

Acousto-Ultrasonic Input-Output Characterization of Unidirectional Fiber Composite Plate by SH Waves

James H. Williams, Jr., and Peter Liao

GRANT NAG3-328
AUGUST 1987

NASA

NASA Contractor Report 4087

Acousto-Ultrasonic Input-Output Characterization of Unidirectional Fiber Composite Plate by SH Waves

James H. Williams, Jr., and Peter Liao
Massachusetts Institute of Technology
Cambridge, Massachusetts

Prepared for
Lewis Research Center
under Grant NAG3-328

National Aeronautics
and Space Administration

**Scientific and Technical
Information Office**

1987

ABSTRACT

A unidirectional fiberglass epoxy composite plate specimen is modelled as a homogeneous transversely isotropic continuum plate medium. Acousto-ultrasonic non-contact input-output characterization by tracing SH waves in the continuum is studied theoretically with a transmitting and a receiving transducer located on the same face of the plate.

The single reflection problem at a stress-free plane boundary in a semi-infinite transversely isotropic medium whose isotropic plane is parallel to the plane boundary is analyzed first. It is found that an incident SH wave results in a reflected SH wave only; the amplitude ratio of the reflected SH wave to the incident SH wave is negative one; and the angle of reflection of the reflected SH wave is equal to the angle of incidence of the incident SH wave. The balance in energy flux normal to the plane boundary is also checked.

The delay time is calculated as if the SH waves were propagating in an infinite half space. It is found that the directional dependence of the phase velocity of the SH waves travelling in the transversely isotropic medium has a significant effect on the delay time, as opposed to the directional independence of the phase velocity of the SH wave travelling in an isotropic medium.

The displacement associated with the SH wave in the plate detected by the non-contact receiving transducer is approximated by an asymptotic solution for an infinite transversely isotropic medium subjected to a harmonic point load. The polar diagrams for the directivity function of the shear stress due to SH waves in the plate are shown at frequencies of 0.75, 1.50 and 2.25 MHz. To maximize signal detection, the transverse transmitting transducer should be placed such that the applied force generated by it is in the direction perpendicular to the line connecting the transmitting and the receiving transducers. This study enhances the quantitative understanding of acousto-ultrasonic nondestructive evaluation (NDE) parameters such as the stress wave factor (SWF) and wave propagation in fiber reinforced composites or any other materials which can be modelled as transversely isotropic media.

INTRODUCTION

Fiber reinforced composite materials are attractive materials for aerospace applications because of their high specific mechanical properties. It has been shown that many composites, such as the unidirectional fiberglass epoxy composites or fiber reinforced ceramics, as shown in Fig. 1, may be modelled as a homogeneous transversely isotropic continuum [1]. In this work, acousto-ultrasonic (AU) noncontact input-output characterization of a homogeneous transversely isotropic elastic plate is investigated by tracing SH waves.

First, single reflection problem of an incident SH wave at a stress-free plane boundary in a semi-infinite transversely isotropic medium whose isotropic plane is parallel to the plane boundary is considered. At such boundaries, the conditions for the existence of wave mode conversion, the angle of reflection of the reflected wave, and the amplitude ratio of the reflected wave to the incident wave are derived.

Second, the SH wave input-output relations are derived when multiple reflections occur at the top and bottom faces of the plate. The delay time between input and output versus the distance separating the transmitting and receiving transducers is analyzed. The directivity function of the shear stress associated with the SH waves is computed.

And, the output displacement at the non-contact receiving transducer is approximated by an asymptotic solution.

This investigation should enhance the quantitative understanding of AU NDE parameter such as the stress wave factor. It also provides the potential for assisting in the development of better NDE schemes utilizing the SWF.

SINGLE REFLECTION PROBLEM AT A STRESS-FREE PLANE BOUNDARY IN SEMI-INFINITE TRANSVERSELY ISOTROPIC MEDIUM WHOSE ISOTROPIC PLANE IS PARALLEL TO PLANE BOUNDARY FOR INCIDENT SH WAVE

1. Reflected SH Wave

For a homogeneous linearly elastic transversely isotropic continuum, the number of independent elastic constants is five [1]. Define a coordinate system (x, y, z) for a semi-infinite transversely isotropic medium whose isotropic plane is parallel to the plane boundary where the reflection occurs as follows: the plane boundary contains the x and y axes, and the z axis is the zonal axis of the medium, which is in the direction parallel to the fiber direction shown in Fig. 1, as shown in Fig. 2. The generalized Hooke's law is written, relative to the (x, y, z) coordinate system, as [1]:

$$
\begin{aligned}
\tau_{xx} &= C_{11}u,x + C_{12}v,y + C_{13}w,z \\
\tau_{yy} &= C_{12}u,x + C_{11}v,y + C_{13}w,z \\
\tau_{zz} &= C_{13}u,x + C_{13}v,y + C_{33}w,z \\
\tau_{xz} &= C_{44}(u,z + w,x) \\
\tau_{yz} &= C_{44}(v,z + w,y) \\
\tau_{xy} &= C_{66}(u,y + v,x)
\end{aligned}
\qquad (1)
$$

where τ_{rs} (r, s = x, y and z) are the normal (r = s) and shear (r ≠ s) stresses with respect to the coordinate system (x, y, z); u, v and w are the displacement components of a point in the medium along the x, y and z axes, respectively; "," denotes partial differentiation with respect to the variable which follows; and C_{11}, C_{12}, C_{13}, C_{33}, and C_{44} are the five independent elastic constants where $C_{66} = 1/2(C_{11} - C_{12})$.

Let a plane progressive wave be represented as [2]

$$(u, v, w) = A\,(P_x, P_y, P_z)\exp\{i\omega(S_x x + S_y y + S_z z - t)\} \qquad (2)$$

where S_x, S_y and S_z are the components of the slowness vector, which is in the same direction as the normal to the wavefront and whose magnitude is equal to the reciprocal of the magnitude of the phase velocity [1], along the x,y and z axes, respectively; P_x, P_y and P_z are the components of a unit vector of particle displacement along the x, y, and z axes, respectively; A is the amplitude of particle displacement; t denotes time and ω denotes radian frequency. It follows from Eqs. (1) and (2) that the stresses can be represented as

$$\begin{aligned}
\tau_{xx} &= i\omega A[C_{11}S_xP_x + C_{12}S_yP_y + C_{13}S_zP_z]\exp\{i\omega(S_xx + S_yy + S_zz - t)\}\\
\tau_{yy} &= i\omega A[C_{12}S_xP_x + C_{11}S_yP_y + C_{13}S_zP_z]\exp\{i\omega(S_xx + S_yy + S_zz - t)\}\\
\tau_{zz} &= i\omega A[C_{13}S_xP_x + C_{13}S_yP_y + C_{33}S_zP_z]\exp\{i\omega(S_xx + S_yy + S_zz - t)\}\\
\tau_{xz} &= i\omega A[C_{44}S_zP_x + C_{44}S_xP_z]\exp\{i\omega(S_xx + S_yy + S_zz - t)\} \qquad (3)\\
\tau_{yz} &= i\omega A[C_{44}S_zP_y + C_{44}S_yP_z]\exp\{i\omega(S_xx + S_yy + S_zz - t)\}\\
\tau_{xy} &= i\omega A[C_{66}S_yP_x + C_{66}S_xP_y]\exp\{i\omega(S_xx + S_yy + S_zz - t)\}
\end{aligned}$$

The stress boundary conditions on the stress-free plane boundary

require that [2]

$$\tau_{xz}^{(I)} + \tau_{xz}^{(R)} = 0$$

$$\tau_{yz}^{(I)} + \tau_{yz}^{(R)} = 0 \qquad (4)$$

$$\tau_{zz}^{(I)} + \tau_{zz}^{(R)} = 0$$

where $\tau_{rz}^{(I)}$ (r=x, y and z) represents stresses on the plane boundary associated with the incident wave, and $\tau_{rz}^{(R)}$ (r = x, y and z) represents stresses on the plane boundary associated with the reflected waves. In order to satisfy Eq. (4), it is required [2] that the frequency, ω, of the reflected waves be equal to that of the incident wave and that

$$S_x^{(I)} = S_x^{(R)}$$
$$S_y^{(I)} = S_y^{(R)}. \qquad (5)$$

As a result of Eq. (5), the slowness vectors of the incident and reflected waves lie in a plane called the plane of incidence. This analysis can be simplified by assuming that the slowness vectors of the incident and reflected waves are in the plane x = 0, as shown in Fig. 2. Since the slowness vectors of the incident and reflected waves are in the plane x = 0,

$$S_x^{(I)} = S_x^{(R)} = 0. \qquad (6)$$

It has been shown that an SH wave with slowness vector in a plane containing the zonal axis of a transversely isotropic medium possesses a transverse displacement; that is, for the coordinates in Fig. 2, $(P_x, P_y, P_z) = (1, 0, 0)$ [3]. It follows from Eqs. (3) and (6) that the stresses associated with SH waves are

$$\begin{gathered} \tau_{xx} = \tau_{yy} = \tau_{zz} = \tau_{yz} = 0 \\ \tau_{xz} \neq 0 \; ; \quad \tau_{xy} \neq 0. \end{gathered} \tag{7}$$

It has also been shown [3] that an SV wave and a P wave with slowness vector in a plane containing the zonal axis of the transversely isotropic medium are quasi-transverse and quasi-longitudinal, respectively; the component of the unit vector of particle displacement for SV and P waves along the x axis, P_x, vanishes, whereas the components along the y and z axes, P_y and P_z, do not. It follows from Eqs. (3) and (6) that stresses associated with P and SV waves are

$$\begin{gathered} \tau_{xy} = \tau_{xz} = 0 \\ \tau_{yz} \neq 0 \; ; \; \tau_{xx} \neq 0 \; ; \; \tau_{yy} \neq 0 \; ; \; \tau_{zz} \neq 0. \end{gathered} \tag{8}$$

Assume that an SH wave is incident on the plane boundary, the x-y plane in Fig. 2. It follows from Eqs. (4) and (7) that

$$\tau_{xz}^{(I)} = \tau_{zz}^{(I)} = 0$$
$$\tau_{xz}^{(I)} \neq 0. \tag{9}$$

As a result of Eq.(9), it is known from Eq. (4) that $\tau_{yz}^{(R)}$ and $\tau_{zz}^{(R)}$ are equal to zero. This means that no P or SV waves will be reflected back into the medium because a reflected wave of either the P or SV type results in nonzero values of the stresses τ_{yy} and τ_{zz}. It follows from Eq. (4) that

$$\tau_{xz}^{(I)} + \tau_{xz}^{(R)} = 0 \tag{10}$$

Since a reflected SH wave results in nonzero values of shear stresses, τ_{xz} and τ_{xy}, it is therefore concluded that only an SH wave will be reflected back into the medium.

2. Slowness Surface for SH Wave

The equations of motion relative to the coordinate system (x,y,z) are [2]

$$\begin{aligned} \tau_{xx,x} + \tau_{xy,y} + \tau_{xz,z} &= \rho u,tt \\ \tau_{xy,x} + \tau_{yy,y} + \tau_{yz,z} &= \rho v,tt \\ \tau_{xz,x} + \tau_{yz,y} + \tau_{zz,z} &= \rho w,tt \end{aligned} \tag{11}$$

It follows from Eqs. (1), (2) and (11) that the following equations of motion are obtained:

$$
\begin{aligned}
&[C_{11}S_x^2 + C_{66}S_y^2 + C_{44}S_z^2 - \rho]P_x + (C_{12} + C_{66})S_xS_yP_y \\
&\qquad + (C_{13} + C_{44})S_xS_zP_z = 0 \\
&(C_{12} + C_{66})S_xS_yP_x + [C_{66}S_x^2 + C_{11}S_y^2 + C_{44}S_z^2 - \rho]P_y \\
&\qquad + (C_{13} + C_{44})S_yS_zP_z = 0 \\
&(C_{13} + C_{44})S_xS_zP_x + (C_{13} + C_{44})S_yS_zP_y + [C_{44}(S_x^2 + S_y^2) \\
&\qquad + C_{33}S_z^2 - \rho]P_z = 0
\end{aligned}
\tag{12}
$$

The condition of the plane wave solution is expressed by setting the determinant of the matrix of the coefficients of P_x, P_y and P_z in Eq. (12) equal to zero [1]:

$$
\begin{vmatrix}
[C_{11}S_x^2 + C_{66}S_y^2 + C_{44}S_z^2 - \rho] & (C_{12} + C_{66})S_xS_y & (C_{13} + C_{44})S_xS_z \\
(C_{12} + C_{66})S_xS_y & [C_{66}S_x^2 + C_{11}S_y^2 + C_{44}S_z^2 - \rho] & (C_{13} + C_{44})S_yS_z \\
(C_{13} + C_{44})S_xS_z & (C_{13} + C_{44})S_yS_z & [C_{44}(S_x^2 + S_y^2) + C_{33}S_z^2 - \rho]
\end{vmatrix} = 0
\tag{13}
$$

Expanding Eq. (13), we obtain three sheets of slowness surface. The slowness surface for an SH wave is [3]

$$
C_{66}(S_x^2 + S_y^2) + C_{44}S_z^2 = \rho \ . \tag{14}
$$

In the present study, the slowness vectors of the incident and reflected SH waves are confined to the y-z plane, as shown in Fig. 2. The intersection of the slowness surface with the plane x=0 is given by [3] as

$$\frac{C_{66}}{\rho} S_y^2 + \frac{C_{44}}{\rho} S_z^2 = 1. \qquad (15)$$

The numerical values of the constants C_{44}, C_{66} and ρ for the fiberglass epoxy composite shown in Fig. 1 are given in [1] as $C_{44} = 4.422 \times 10^9$ N/m^2, $C_{66} = 3.243 \times 10^9$ N/m^2, and $\rho = 1850$ kg/m^3. One quadrant of the slowness surface for an SH wave travelling in the fiberglass epoxy composite is obtained by substituting the numerical values of the elastic constants and the density into Eq. (15), and is shown in Fig. 3.

3. Angle of Reflection

It follows from Eq. (5) that the component of the slowness vector of an incident SH wave along the y axis, $S_y^{(I)}$, is equal to that of the reflected SH wave, $S_y^{(R)}$. As result of Eqs. (5) and (15), the relationship between the z-components of the slowness vectors of an incident SH wave and the reflected SH wave is

$$S_z^{(I)} = - S_z^{(R)}. \tag{16}$$

The minus sign is due to the fact that the slowness vector of an incident SH wave points out of the medium, whereas the slowness vector of the reflected SH wave points into the medium, as shown in Fig. 2. Consequently, the value of the z-component of the slowness vector of an incident SH wave, $S_z^{(I)}$, is negative, whereas that of the reflected wave, $S_z^{(R)}$, is positive.

The angle of reflection is defined as the angle between the slowness vector of a reflected SH wave and the normal to the plane boundary where the reflection occurs. Similarly, the angle of incidence is defined as the angle between the slowness vector of an incident SH wave and the normal to the plane boundary, as shown in Fig. 2. Therefore, the angle of reflection of a reflected SH wave is

$$\theta_R = \tan^{-1}(S_y^{(R)}/S_z^{(R)}) \tag{17}$$

and the angle of incidence of an incident SH wave is

$$\theta_R = \tan^{-1}(S_y^{(I)}/-S_z^{(I)}). \tag{18}$$

It follows from Eqs. (5), (16), (17) and (18) that the angle of incidence is equal to the angle of reflection, as shown in Fig. 2.

4. Amplitude Ratio of Reflected Wave to Incident Wave

The amplitude ratio of the reflected SH wave to the incident SH wave can be computed from the boundary condition on the stresses, Eq. (4). Assume an SH wave of unit amplitude travelling in the plane $x = 0$ is incident on the plane boundary at the origin, as shown in Fig. 2. The shear stress, $\tau_{xz}^{(I)}$, associated with the incident SH wave on the plane boundary can be obtained from Eqs. (3) and (6) as

$$\tau_{xz}^{(I)} = i\omega C_{44} S_z^{(I)} \quad . \tag{19}$$

Similarly, the shear stress, $\tau_{xz}^{(R)}$, associated with the reflected SH wave on the plane boundary is

$$\tau_{xz}^{(R)} = i\omega A^{(R)} C_{44} S_z^{(R)} . \tag{20}$$

It follows from Eqs. (10), (16), (19) and (20) that the amplitude of the reflected SH wave is

$$A^{(R)} = -1. \tag{21}$$

Therefore, the amplitude ratio of the reflected SH wave to the incident SH wave is negative one.

5. Balance in Energy Flux Normal to Plane Boundary

The balance in energy flux normal to the plane boundary must be satisfied and is expressed as [3]

$$F_z^{(I)} + F_z^{(R)} = 0 \tag{22}$$

where $F_z^{(I)}$ and $F_z^{(R)}$ are the components of the energy fluxes of the incident and the reflected SH waves along the z axis, respectively.

The component of the energy flux associated with an SH wave along the z axis is [4]

$$F_z = C_{44}A^2\omega^2 S_z \ . \tag{23}$$

It follows from Eqs. (16), (21) and (23) that the sum of the z-component of the energy flux of the incident SH wave and that of the reflected SH wave is equal to zero. Accordingly, the requirement for the balance in energy flux perpendicular to the plane boundary where a reflection occurs, Eq. (22), is satisfied.

The z-components of the energy flux of an incident SH wave of unit amplitude and the reflected SH wave, Eq. (23), in the semi-infinite transversely isotropic medium are shown in Fig. 4, exclusive

of the radian frequency ω, as functions of the angle of incidence with the numerical value of the elastic constant C_{44} given in [1] for the unidirectional fiberglass epoxy composite shown in Fig.1 as $C_{44} = 4.422 \times 10^9$ N/m^2. The balance in energy flux normal to the plane boundary, Eq. (22), is also shown in Fig. 4, which is independent of frequency.

ACOUSTO-ULTRASONIC NON-CONTACT INPUT-OUTPUT CHARACTERIZATION OF FIBERGLASS EPOXY COMPOSITE PLATE

It has been shown [1] that the unidirectional fiberglass epoxy composite shown in Fig. 1 may be modelled as a homogeneous transversely isotropic continuum. For the axes shown in Fig. 1, the isotropic plane of equivalent continuum lies in the midplane of the plate [1]. A cartesian coordinate system (x, y, z) is chosen so that the x-y plane is the isotropy plane; thus, the upper and lower surfaces of the plate are at z= h/2 and z= -h/2, respectively, where h is the plate thickness. The properties of the equivalent continuum model of the unidirectional fiberglass epoxy composite plate are [1]

$$
\begin{aligned}
h &= 0.1 \text{ m} \\
C_{11} &= 10.581 \times 10^9 \text{ N/m}^2 \\
C_{12} &= 4.679 \times 10^9 \text{ N/m}^2 \\
C_{13} &= 40.741 \times 10^9 \text{ N/m}^2 \\
C_{33} &= 4.422 \times 10^9 \text{ N/m}^2 \\
C_{44} &= 3.243 \times 10^9 \text{ N/m}^2 \\
\rho &= 1850 \text{ kg/m}^3
\end{aligned}
\tag{24}
$$

Non-contact transmitting and receiving transducers are located on the same face of a fiberglass epoxy composite plate specimen, as shown in Fig. 5. The unidirectional fiberglass epoxy composite plate spe-

cimen is considered as a plate of thickness h and of infinite planar (x-y) extent. The input electrical voltage to the transmitting transducer is $V_i(t)$ and the output electrical voltage from the receiving transducer is $V_o(t)$ where t represents time. The transmitting transducer converts an input electrical voltage into a stress, whereas the receiving transducer converts a stress associated with stress waves travelling in the plate into an output voltage. In the following analysis, only the SH waves are traced. The SH waves which are generated by the transmitting transducer located above point O experience multiple reflections at each face of the plate, and then reach the receiving transducer located above point M, as shown in Fig. 6. Since the isotropic plane lies in the midplane and is parallel to both the top and the bottom faces where multiple reflections occur, the angle of reflection of the reflected SH wave is equal to the angle of incidence of an incident SH wave for each reflection at each face of the plate. Accordingly, the SH wave travelling from the input O to the output M may be considered as waves propagating in a semi-infinite transversely isotropic medium and travelling to point M' as if there were no bottom face, as shown in Fig. 6.

1. Delay Time and Phase Velocity

Let the input O and the output M lie in the y-z plane. Assume the number of reflections at the bottom face experienced by the SH

wave in travelling from the input O to the output M is n, as shown in Fig. 6. With respect to the z axis, the angle of incidence of the SH wave at each face of the plate is θ, and the total distance travelled by the wave is R_n. From the geometry in Fig. 6,

$$\theta = \tan^{-1}(\ell/2nh) \tag{25}$$

where ℓ is the separation distance between the input O and the output M, and

$$R_n = \ell/\sin\theta . \tag{26}$$

The delay time t_n for the wave to reach the receiving transducer is

$$t_n = R_n/C_1(\theta) \tag{27}$$

where $C_1(\theta)$ is the directionally dependent phase velocity of the SH wave, and which for the unidirectional fiberglass epoxy composite plate is [1]

$$C_1(\theta) = [(C_{66}\sin^2\theta + C_{44}\cos^2\theta]^{1/2} \tag{28}$$

where C_{44}, C_{66} and ρ are given by Eq. (24).

The phase velocity C_1 as a function of the angle of incidence θ is shown in Fig. 7. The delay time is then computed when the number of reflections n at the bottom face of the plate is equal to 10, 100, 300 or 500. The numerical results are shown in Fig. 8 where the delay time t_n is plotted as the ordinate, and the dimensionless quantity ℓ/h is plotted as the abscissa for values of zero to 300.

2. Displacement Detected By the Receiving Transducer

The displacement detected by the non-contact receiving transducer above point M, radiated by the transverse transmitting transducer, is assumed to be equivalent to the displacement at point M', associated with the SH wave propagating in a semi-infinite transversely isotropic medium. Except for the reflection coefficients at each face (to be discussed later), the displacement is computed as if there were no bottom boundary, as shown in Fig. 6. The shear stress at point M' is approximated by the far-field asymptotic solution for large R_n of an infinite transversely isotropic medium subjected to a harmonic point load.

Now consider an infinite transversely isotropic medium in which the z axis of a rectangular cartesian system O(x,y,z) is the zonal axis of the medium and the x-y plane coincides with the isotropic plane, as shown in Fig. 9. The equations of motion including the

body force are [5]

$$\tau_{xx,x} + \tau_{xy,y} + \tau_{xz,z} + \rho X = \rho u,tt \tag{29}$$

$$\tau_{xy,x} + \tau_{yy,y} + \tau_{yz,z} + \rho Y = \rho v,tt \tag{30}$$

$$\tau_{xz,x} + \tau_{yz,y} + \tau_{zz,z} + \rho Z = \rho w,tt \tag{31}$$

where τ_{rs} (r, s = x, y, z) are the normal (r = s) and shear ($r \neq s$) stresses with respect to the chosen coordinate system O(x, y, z); u, v and w are displacement components of a point in the medium along the x, y and z axes, respectively; X, Y and Z are the components of the body force along the x, y and z axes respectively; ρ is the density; t is time; and "," denotes partial differentiation with respect to the variable which follows.

If we differentiate Eq. (30) with respect to x and Eq. (29) with respect to y, we find upon substitution of the resulting equations and using the appropriate stress-strain relations, Eq. (1), that

$$\Lambda,tt = \frac{C_{66}}{\rho}(\Lambda,xx + \Lambda,yy) + \frac{C_{44}}{\rho}\Lambda,zz + Y,x - X,y \tag{32}$$

where $\Lambda = v,x - u,y$.

For a harmonic point load at the origin, we take body forces of the form

$$\begin{aligned} X &= X_o\delta(x)\delta(y)\delta(z)e^{-i\omega t} \\ Y &= Y_o\delta(x)\delta(y)\delta(z)e^{-i\omega t} \\ Z &= Z_o\delta(x)\delta(y)\delta(z)e^{-i\omega t} \end{aligned} \tag{33}$$

where $\delta(r)$ $(r = x, y, z)$ are the Dirac delta functions and X_o, Y_o and Z_o are the magnitude of the respective point body forces. Λ can be expressed as a threefold Fourier integral [5]

$$\Lambda(x,y,z,t) = \int_{-\infty}^{\infty}\int\int\int \bar{\Lambda}(S_x,S_y,S_z,t)\ \exp\{i\omega(S_x x+S_y y+S_z z-t)\}dS_x dS_y dS_z \tag{34}$$

where

$$\bar{\Lambda}(S_x,S_y,S_z,t) = 1/8\pi^3 \int_{-\infty}^{\infty}\int\int\int \Lambda(x,y,z,t)\ \exp\{i\omega(-S_x x-S_y y-S_z z+t)\}dxdydz.$$

Similarly, Y,x and X,y can be expressed as threefold Fourier integrals

$$\begin{aligned} Y,x &= i\omega S_x \int_{-\infty}^{\infty}\int\int\int \bar{Y}\ \exp\{i\omega(S_x x+S_y y+S_z z-t)\}dS_x dS_y dS_z \\ X,y &= i\omega S_y \int_{-\infty}^{\infty}\int\int\int \bar{X}\ \exp\{i\omega(S_x x+S_y y+S_z z-t)\}dS_x dS_y dS_z \end{aligned} \tag{35}$$

where

$$\bar{X} = 1/8\pi^3 \iiint_{-\infty}^{\infty} X_o \delta(x)\delta(y)\delta(z) e^{-i\omega t}$$

$$\exp\{i\omega(S_x x + S_y y + S_z z - t)\} dS_x dS_y dS_z$$

$$= X_o/8\pi^3$$

and, similarly,

$$\bar{Y} = Y_o/8\pi^3; \quad \bar{Z} = Z_0/8\pi^3.$$

It follows from Eqs. (32), (33), (34) and (35) that

$$\bar{\Lambda} = \frac{i(S_x Y_o - S_y X_o)}{8\pi^3 \omega G(S_x, S_y, S_z)} \tag{36}$$

where $G(S_x, S_y, S_z) = C_{66}/\rho(S_x^2 + S_y^2) + C_{44}/\rho S_z^2 - 1.$

Therefore, $G(S_x, S_y, S_z) = 0$ represents the slowness surface for an SH wave by comparison with Eq. (14). As a result of Eqs. (34) and (36), Λ becomes

$$\Lambda(x,y,z,t) = \iiint_{-\infty}^{\infty} \frac{iS_x Y_o - iS_y X_o}{8\pi^3 \omega G(S_x, S_y, S_z)}$$

$$\exp\{i\omega(S_x x + S_y y + S_z z - t)\} dS_x dS_y dS_z \tag{37}$$

The asymptotic solution at large distance from the point load is obtained by applying the theory of residues, the method of stationary phase, and the radiation condition [5] as

$$\Lambda(x,y,z,t) - \frac{i\omega(S_x^* Y_o - S_y^* X_o)}{2\pi R|\nabla G|(|K_G|)^{1/2}} \exp\{i\omega(S_x^* x + S_y^* y + S_z^* z - t)\} \qquad (38)$$

where (S_x^*, S_y^*, S_z^*) are the points on the slowness surface for an SH wave, $G(S_x, S_y, S_z) = 0$, where the normal is parallel to the OP direction; R is the distance from the origin O where the point load is applied to the point of interest P in the medium; ∇G is the gradient of $G(S_x, S_y, S_z)$ and $|\nabla G|$ is the magnitude of the gradient of $G(S_x, S_y, S_z)$ and is expressed as

$$|\nabla G| = [G,S_x + G,S_y + G,S_z]^{1/2} \qquad (39)$$

and is evaluated at points (S_x^*, S_y^*, S_z^*) of the slowness surface for an SH wave, $G(S_x, S_y, S_z) = 0$, where the normal is parallel to the OP direction; K_G is the gaussian curvature of the slowness surface for an SH wave and is expressed as

$$K_G = \frac{1}{(G_{,S_x}^2 + G_{,S_y}^2 + G_{,S_z}^2)} \left[\Sigma\{G_{,S_z}^2 (G_{,S_x S_x}\, G_{,S_y S_y} - G_{,S_x S_y}^2) + 2G_{,S_x}\, G_{,S_y}(G_{,S_x S_z}\, G_{,S_y S_z} - G_{,S_x S_y}\, G_{,S_z S_z})\} \right] \quad (40)$$

where Σ is the sum with respect to cyclic permutation of S_x, S_y and S_z, and $(|K_G|)^{1/2}$ is the square root of the magnitude of the gaussian curvature of the slowness surface, $G(S_x, S_y, S_z) = 0$, and is evaluated at points (S_x^*, S_y^*, S_z^*) of the slowness surface where the normal is parallel to the OP direction, as shown in Fig. 9.

The displacement component along the x and y axes, u and v, due to an SH wave can be obtained by direct integration of the definition of Λ in Eq. (32), in conjunction with pages 14 and 15 of [6] and is asymptotically expressed as

$$u(x,y,z,t) \sim \frac{S_y^{*2} X_o - S_x^* S_y^* Y_o}{2\pi R(S_x^{*2} + S_y^{*2})|\nabla G|(|K_G|)^{1/2}} \exp\{i\omega(S_x^* x + S_y^* y + S_z^* z - t) \quad (41)$$

$$v(x,y,z,t) \sim \frac{-S_x^* S_y^* X_o + S_x^{*2} Y_o}{2\pi R(S_x^{*2} + S_y^{*2})|\nabla G|(|K_G|)^{1/2}} \exp\{i\omega(S_x^* x + S_y^* y + S_z^* z - t)$$

It is known from the definition of Λ in Eq. (32) and Eq. (37) that SH waves have no contribution to the displacement component along the z axis, w.

However, it should be noted that there is only one point on the slowness surface, $G(S_x, S_y, S_z) = 0$, where the normal is parallel to a given direction OP. This is because the slowness surface for an SH wave is a spheroid, Eq. (14). Consequently, if (x, y, z) are the coordinates of a given point in the medium, there will be only one SH wavefront passing through it corresponding to a point (S_x^*, S_y^*, S_z^*) on the slowness surface where the normal is parallel to the given direction. Note that in this analysis, it has not been necessary to use Eq. (31).

3. Directivity Function

The shear stress, τ_{xz}, associated with SH waves reaching the point M' in Fig. 6 is given from Eqs. (1) and (41) as

$$\tau_{xz}(x,y,z,t) = -\frac{iC_{44}\omega S_z^*(S_y^{*2}X_o - S_x^*S_y^*Y_o)}{2\pi R(S_x^{*2} + S_y^{*2})|\nabla G|(|K_G|)^{1/2}}$$

$$\exp\{i\omega(S_x^*x + S_y^*y + S_z^*z - t)\} \qquad (42)$$

The directivity function D_{SH} of the shear stress, τ_{xz}, associated with the SH wave is determined from the amplitude of the shear stress in Eq. (42) by setting $X_o = Y_o = R = 1$;

$$D_{SH} = \frac{C_{44}S_z^*|S_y^{*2} - S_x^*S_y^*|\omega}{2\pi(S_x^{*2} + S_y^{*2})|\nabla G|(|K_G|)^{1/2}} \tag{43}$$

Since the point 0 and the point M' in Fig. 6 are located in y-z plane, the evaluation of the directivity function D_{SH} is simplified by setting $S_x = 0$ in Eq. (43).

Due to axial symmetry with respect to the zonal axis, the z axis, of the transversely isotropic medium, the value of the directivity function D_{SH} thus obtained holds for all values of S_x. Therefore, it follows from Eq. (39), (40) and (43) that

$$D_{SH} = \frac{C_{44}\omega S_z^*}{4\pi C_{66}/\rho(C_{44}/\rho)^{1/2}}\left[\left(\frac{C_{66}}{\rho}\ S_y^*\right)^2 + \left(\frac{C_{44}}{\rho}\ S_z^*\right)^2\right]^{1/2} \tag{44}$$

The polar diagrams for the directivity function D_{SH} of the shear stress, τ_{xz}, associated with the SH waves travelling in the unidirectional fiberglass epoxy composite are obtained from Eqs. (24), (25), and (44) at frequencies of 0.75, 1.50 and 2.25 MHz, and are shown in Fig. 10, where the angle of incidence θ, given by Eq. (25), is used to determine the direction in which the value of a point $(0, S_y^*, S_z^*)$ on

the slowness surface where the normal is parallel to the given direction is thus obtained.

4. Assumptions on the Transducers

The non-contact transmitting transducer in Fig. 5 is assumed to transform an electrical voltage into a uniform shear stress; however, the non-contact receiving transducer in Fig. 5 transforms a displacement into an electrical voltage. The approach which follows is similar to that given in [7].

If an input voltage of amplitude V and frequency ω is applied according to

$$V_i(t) = Ve^{-i\omega t} \tag{45}$$

see Fig. 5, the stress σ that is introduced into the specimen by the non-contact transmitting transducer is

$$\sigma(t) = F_1(\omega)Ve^{-i(\omega t + \phi_1)} \tag{46}$$

where $F_1(\omega)$ is the transduction ratio for the transmitting transducer in transforming a voltage to a stress and ϕ_1 is a phase angle. In Eqs. (45) and (46), the harmonic character of the signals is expressed

in the complex notation where $i = \sqrt{-1}$ and only the real parts of these and subsequent equations should be considered. Thus, the amplitude T of the applied force is defined as

$$T = F_1(\omega)V. \tag{47}$$

Similarly, if a stress wave producing a displacement component U and frequency ω that is detected by the non-contact receiving transducer is defined as

$$u(t) = Ue^{i\omega t} \tag{48}$$

the output voltage from the non-contact receiving transducer, see Fig. 5, is

$$V_o(t) = F_2(\omega)U' e^{-i(\omega t + \phi_2)} \tag{49}$$

where $F_2(\omega)$ is the transduction ratio for the non-contact receiving transducer in transforming a displacement to a voltage, and ϕ_2 is a phase angle. Thus, the amplitude V' of the output electrical voltage is

$$V' = F_2(\omega)U. \tag{50}$$

The characteristics of $F_1(\omega)$ and $F_2(\omega)$ are unknown except that the dimension of the product $F_1(\omega)F_2(\omega)$ is $[kg/m^2 \cdot sec^2]$.

5. Steady-State Output Voltage Amplitude due to Multiple Wave Reflections in Plate

Since only the SH waves travelling in the y-z plane are considered in Fig. 6, it follows from Eqs. (26), (39), (40) and (41) that the amplitude of the hypothetical displacement at point M′ is $U_{M'}$, and is defined as

$$U_{M'} = \frac{(C_{44}\rho)^{1/2} S_z^* T}{2\pi R_n (C_{11}-C_{12})} \tag{51}$$

where T represents the magnitude of the shear stress generated by the non-contact transmitting transducer along the direction perpendicular to the line connecting the point 0 and the point M in Fig. 6 and is equivalent to X_o in Eq. (41).

However, with the bottom boundary present, the wave is reflected a total of (2n-1) times, as shown in Fig. 6. Thus, the amplitude of the displacement at point M is U_M, and is obtained by modifying Eq. (51) as

$$U_M = Q_{SHSH}^{2n-1} U_{M'} \tag{52}$$

where Q_{SHSH} is the reflection coefficient of SH waves to SH waves, and its value is -1, as given by Eq. (21).

The amplitude of the output voltage from the non-contact receiving transducer is V' and can be obtained by combining Eqs. (50), (51)and (52) as

$$V' = \frac{F_2(\omega)\ Q_{SHSH}^{2n-1}\ (C_{44}\rho)^{1/2}\ S_z^*\ T}{2\pi\ R_n\ (C_{11}-C_{12})} \tag{53}$$

Substitution of Eq. (47) into Eq. (53) gives

$$V' = \frac{F_1(\omega)\ F_2(\omega) Q_{SHSH}^{2n-1}\ (C_{44}\rho)^{1/2}\ S_z^*\ V}{2\pi\ R_n\ (C_{11}-C_{12})}\ . \tag{54}$$

Introducing the SH wave attenuation constant α of the fiberglass epoxy composite and a possible electrical signal amplification factor K, Eq. (54) can be written as

$$V' = \frac{K\ F_1(\omega)\ F_2(\omega)\ Q_{SHSH}^{2n-1}\ (C_{44}\rho)^{1/2}\ S_z^*\ V\ e^{-\alpha Rn}}{2\pi\ Rn\ (C_{11}-C_{12})}\ . \tag{55}$$

Eq. (55) gives the output voltage amplitude from the non-contact receiving transducer due to an input voltage amplitude V at the non-

contact transmitting transducer when the SH wave path has included n reflections from the bottom face of the fiberglass epoxy composite plate specimen, as shown in Fig. 6.

DISCUSSION AND CONCLUSION

In the acousto-ultrasonic input-output characterization of the unidirectional fiberglass epoxy composite plate, the angle of reflection of the reflected SH wave is equal to the angle of incidence of the incident SH wave for each reflection at either the top or the bottom face of the plate. This is due to the fact that the isotropic plane is parallel to either face of the plate. However, if the parallelism between the isotropic plane and the plane boundaries where reflection occurs does not exist, the angle of reflection is not equal to the angle of incidence. In such a case, the use of a semi-infinite transversely isotropic medium, neglecting the existence of the bottom face of the plate (except for the cumulative reflection coefficients), to compute the delay time t_n and the directivity function D_{SH} becomes inappropriate.

It is observed from Fig. 8 that an increase in the number of reflections n from the bottom face of the plate results in a minor increase in the delay time t_n at each value of dimensionless separation ℓ/h. For a given plate thickness h and a given separation distance ℓ between the transmitting transducer and the receiving transducer, an increase in the number of reflections n results in a decrease in the angle of incidence θ, as given by Eq. (25), thereby increasing the travelling distance R_n, from Eq. (26). The phase

velocity C_1 of an SH wave in the unidirectional fiberglass epoxy composite increases with decreasing angle of incidence θ as shown in Fig. 7. The increase in the travelling distance R_n is partly offset by the increase in the phase velocity C_1 with an increase in the number of reflections n. This accounts for the minor increase in the delay time given by Eq. (27). On the other hand, in an isotropic medium, the phase velocity of a stress wave is directionally independent. Thus, the increase in the delay time t_n caused by an increase in the number of reflections n is solely attributed to the increase in the travelling distance R_n in an isotropic plate. Therefore, it is concluded that the directional dependence of the phase velocity of a stress wave travelling in a transversely isotropic medium has a significant effect on the delay time when conducting acousto-ultrasonic testing.

Now, consider the case of a given number of reflections n. An increase in the separation distance ℓ results in an increase in the travelling distance R_n, as shown in Fig. 6, and an increase in the angle of incidence θ given by Eq. (25). The increasing angle of incidence θ results in the decreasing phase velocity C_1, as shown in Fig. 7. Consequently, the delay time t_n increases sharply as a result of the increasing separation distance ℓ for a given number of reflections n, as shown in Fig. 8. However, as the separation distance ℓ approaches infinity , the phase velocity approaches a limit. Thus,

the increase in the delay time t_n is due solely to the increase in the travelling distance R_n, which is similar to the isotropic medium case.

An examination of Eqs. (41) shows that the y-component displacement v associated with an SH wave travelling in the y-z plane, $S_x = 0$, is zero and the x-component displacement associated with an SH wave travelling in the y-z plane, $S_x = 0$, is attributed solely to the x-component of the applied point load. In other words, the non-contact receiving transducer is unable to detect the displacement component along the line connecting the transmitting and the receiving transducers by tracing SH waves in the plate. Further, the only detectable displacement component which is perpendicular to the normal to both faces of the plate and to the line connecting the transmitting and the receiving transducers (that is, the u displacement) becomes non-detectable if the shear stress introduced by the non-contact transmitting transducer is in the direction parallel to the line connecting the transmitting and the receiving transducers, regardless of how large the stress is. Accordingly, to maximize the displacement detected by the non-contact receiving transducer, the transmitting transducer should be placed such that the shear stress generated by it is in the direction perpendicular to the line connecting the transmitting and the receiving transducers as shown in Fig. 11.

This theoretical investigation provides a step forward in the quantitative understanding of acousto-ultrasonic non-destructive evaluation (NDE) parameters such as the stress wave factor (SWF) in transversely isotropic media. It also provides the potential for assisting in the development of more efficient and more revealing NDE schemes utilizing wave propagation.

REFERENCES

[1] E. R. C. Marques and J. H. Williams, Jr., "Stress Waves in Transversely Isotropic Media," Composite Materials and Nondestructive Evaluation Laboratory, MIT, May 1986.

[2] E. G. Henneke II, "Reflection-Refraction of a Stress Wave at a Plane Boundary between Anisotropic Media," Journal of the Acoustical Society of America, Vol. 51, Part 2, April 1972, pp. 210-217.

[3] M. J. P. Musgrave, "On the Propagation of Elastic Waves in Aeolotropic Media," Proceedings of the Royal Society of London, Series A, Vol. 226, 1954, pp. 339-355.

[4] M. J. P. Musgrave, "Reflection and Refraction of Plane Elastic Waves at a Plane Boundary Between Aeolotropic Media," Journal of Geophysics, Vol. 3, 1960, pp. 406-418.

[5] V. T. Buchwald, "Elastic Waves in Anisotropic Media," Proceedings of the Royal Society, Series A, Vol. 253, 1959, pp. 563-580.

[6] J. H. Williams, Jr., E. R. C. Marques and S. S. Lee, "Wave Propagation in Anisotropic Infinite Medium Due to an Oscillatory Point Source with Application to a Unidirectional Composite Material," Composite Materials and Nondestructive Evaluation Laboratory, MIT, May 1986.

[7] J. H. Williams, Jr., H. Karagulle, and S. S. Lee, "Ultrasonic Input-Output for Transmitting and Receiving Longitudinal Transducers Coupled to Same Face of Isotropic Elastic Plate," Materials Evaluation, Vol. 40, May 1982, pp. 655-662.

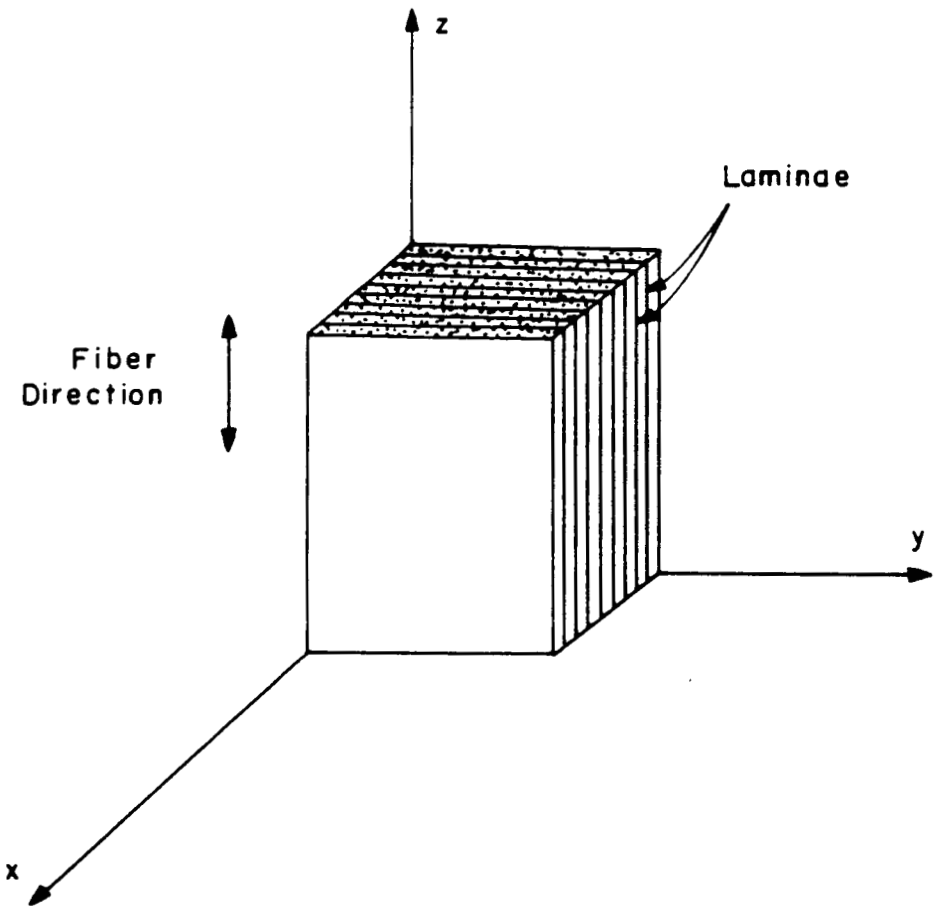

Fig. 1 Unidirectional fiber reinforced composite modelled as transversely isotropic medium.

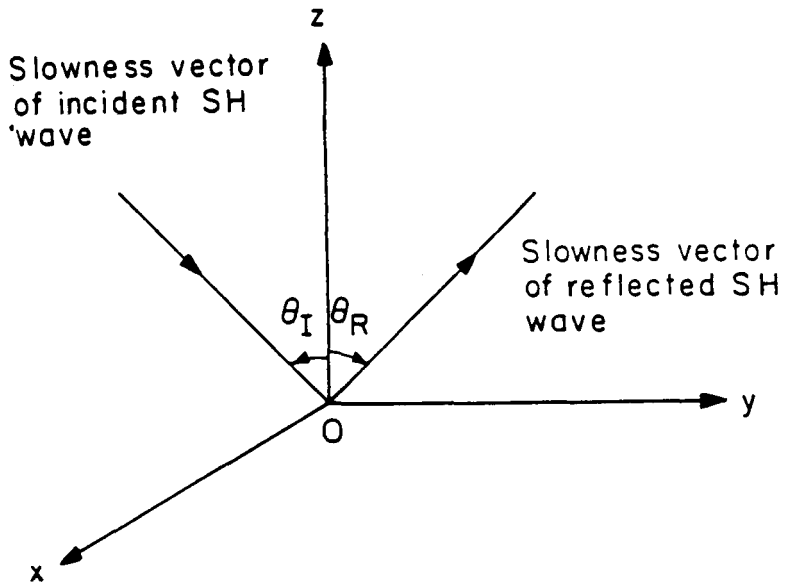

Fig. 2 Coordinate system (x,y,z) in analysis of single reflection problem at stress-free plane boundary of semi-infinite transversely isotropic medium; $z = 0$ is plane boundary where single reflections occurs, $z < 0$ is free space, and $x = 0$ is plane of incidence.

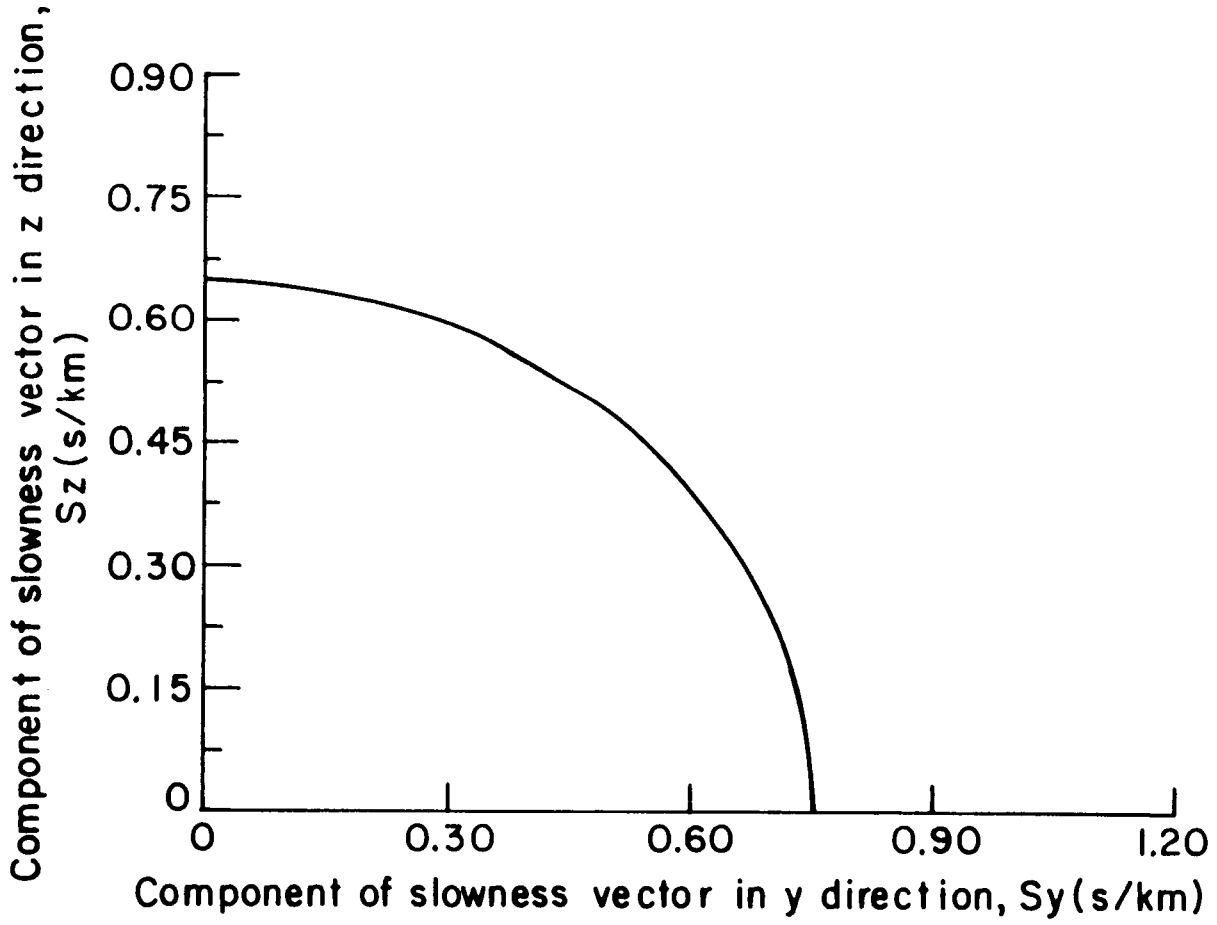

Fig. 3 Slowness surface for SH wave in unidirectional fiberglass epoxy composite for positive y-z quadrant.

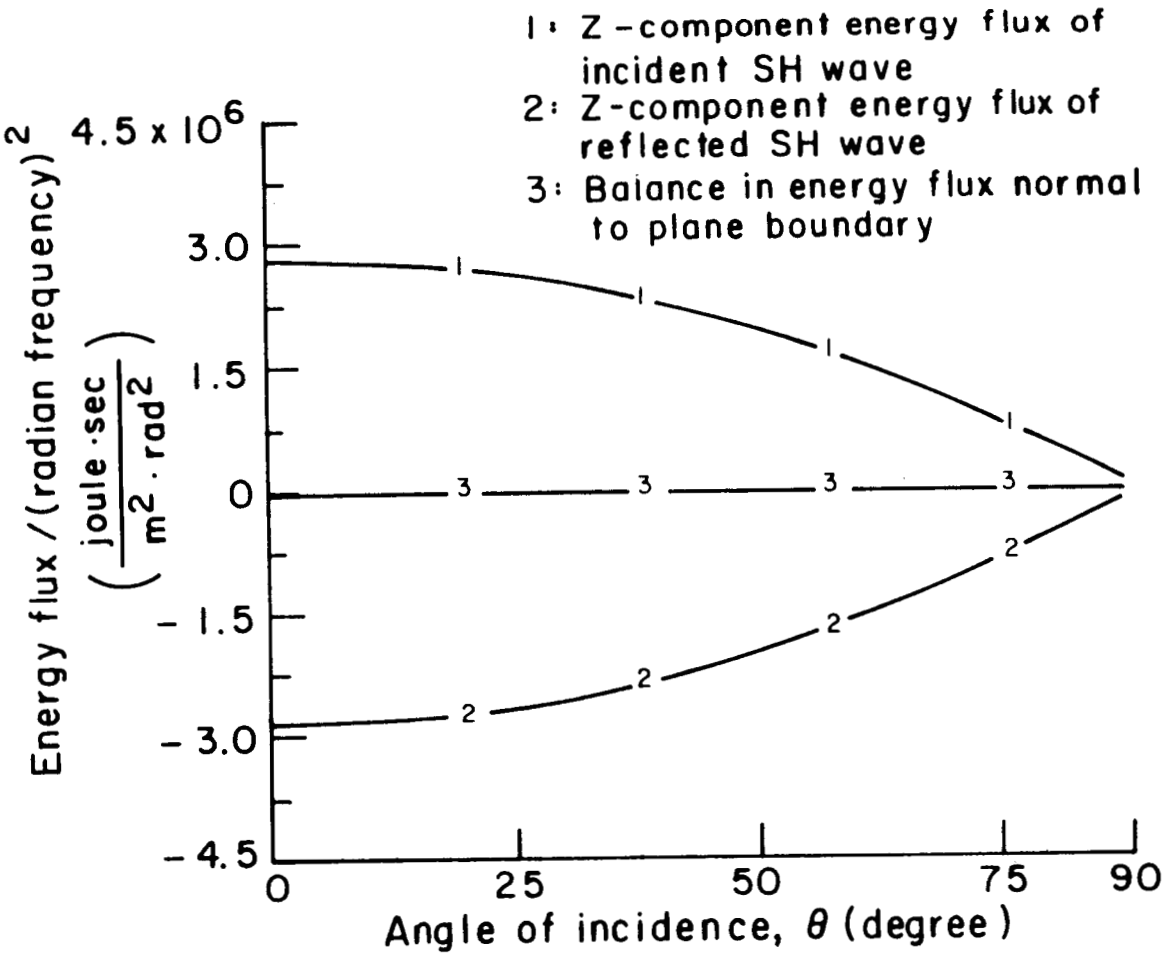

Fig. 4 Energy fluxes normal to plane boundary, exclusive of radian frequency, of incident and reflected SH waves in unidirectional fiberglass epoxy composite.

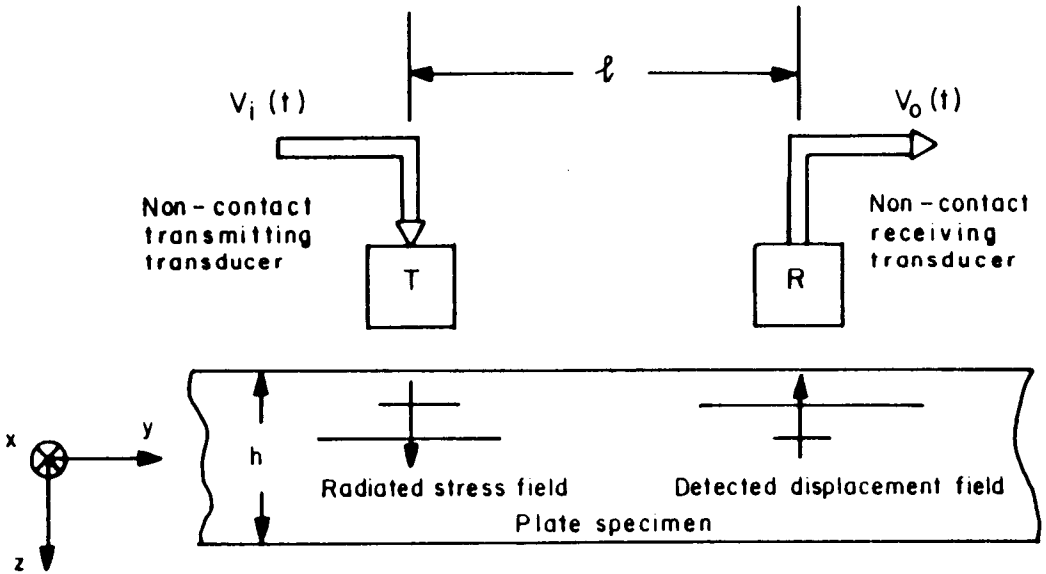

Fig. 5 Schematic of non-contact acousto-ultrasonic test configuration.

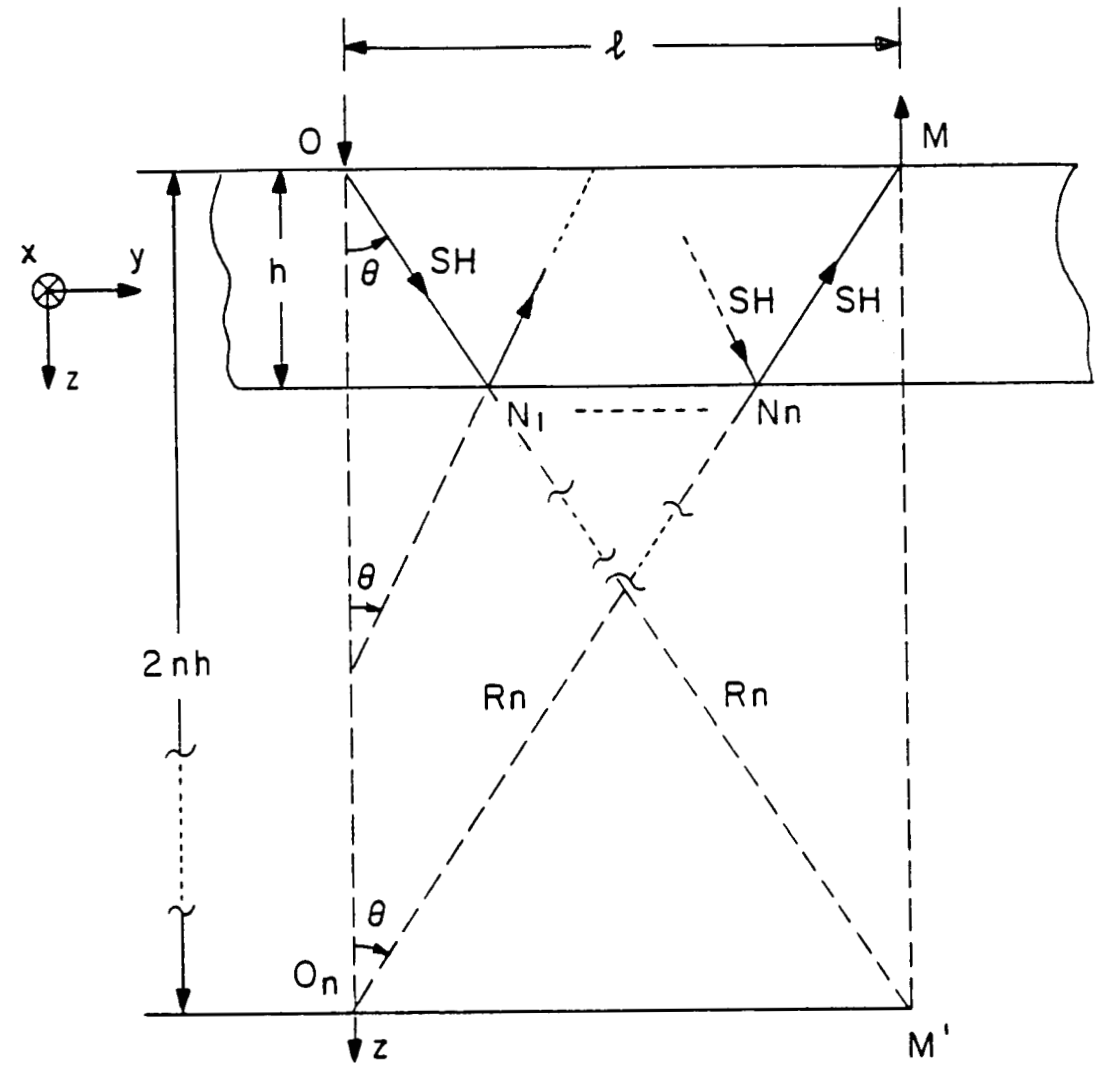

Fig. 6 Path of SH - SH - ... wave which arrives at point M after n reflections from bottom boundary.

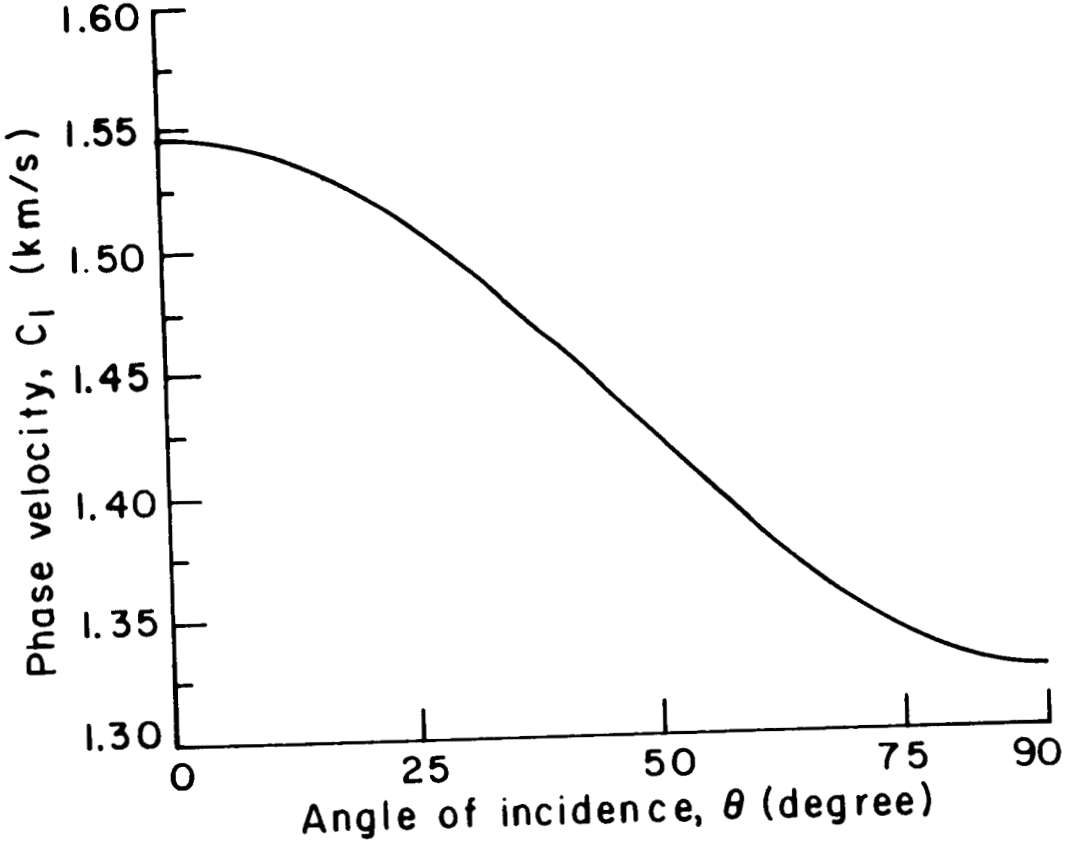

Fig. 7 Phase velocity versus angle of incidence for SH wave travelling in unidirectional fiberglass epoxy composite plate.

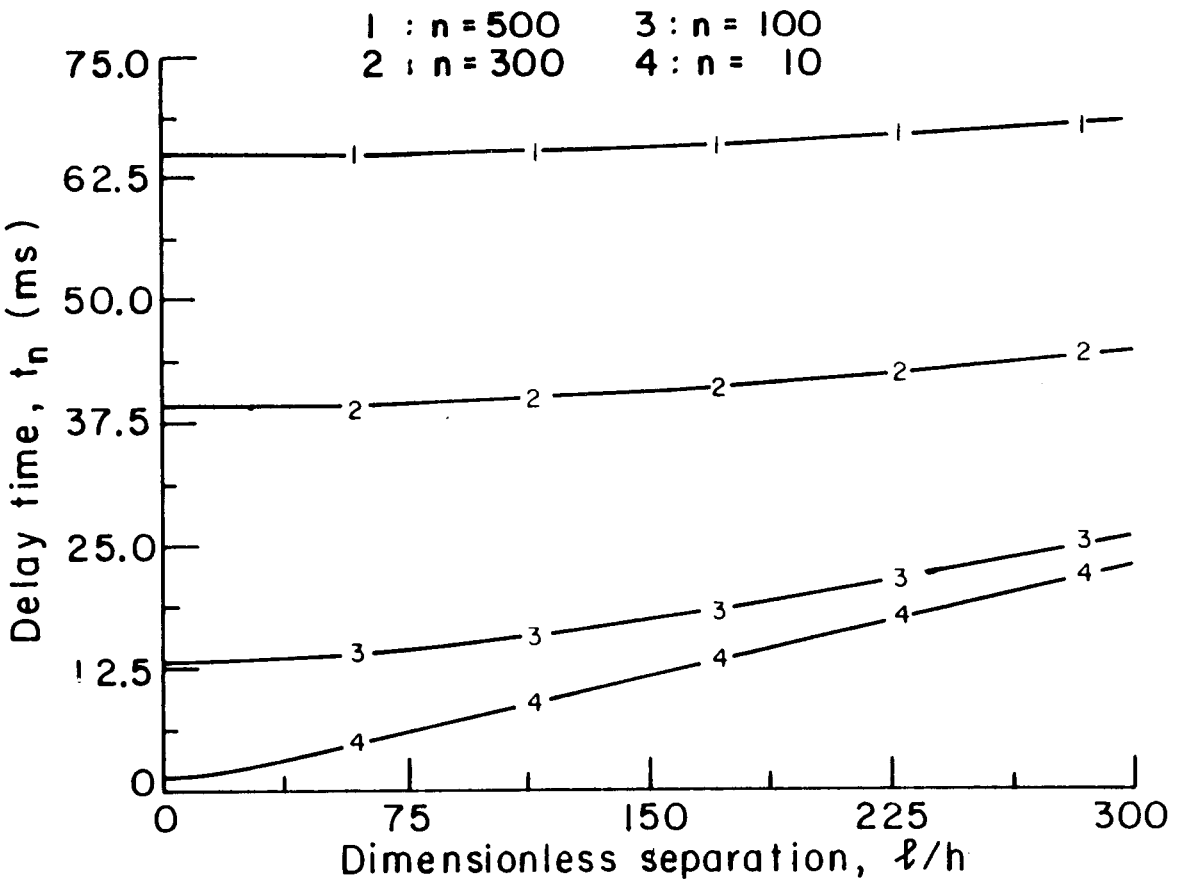

Fig. 8 Delay time versus dimensionless separation ℓ/h with number of reflections n from bottom face of unidirectional fiberglass epoxy composite plate specimen as parameter.

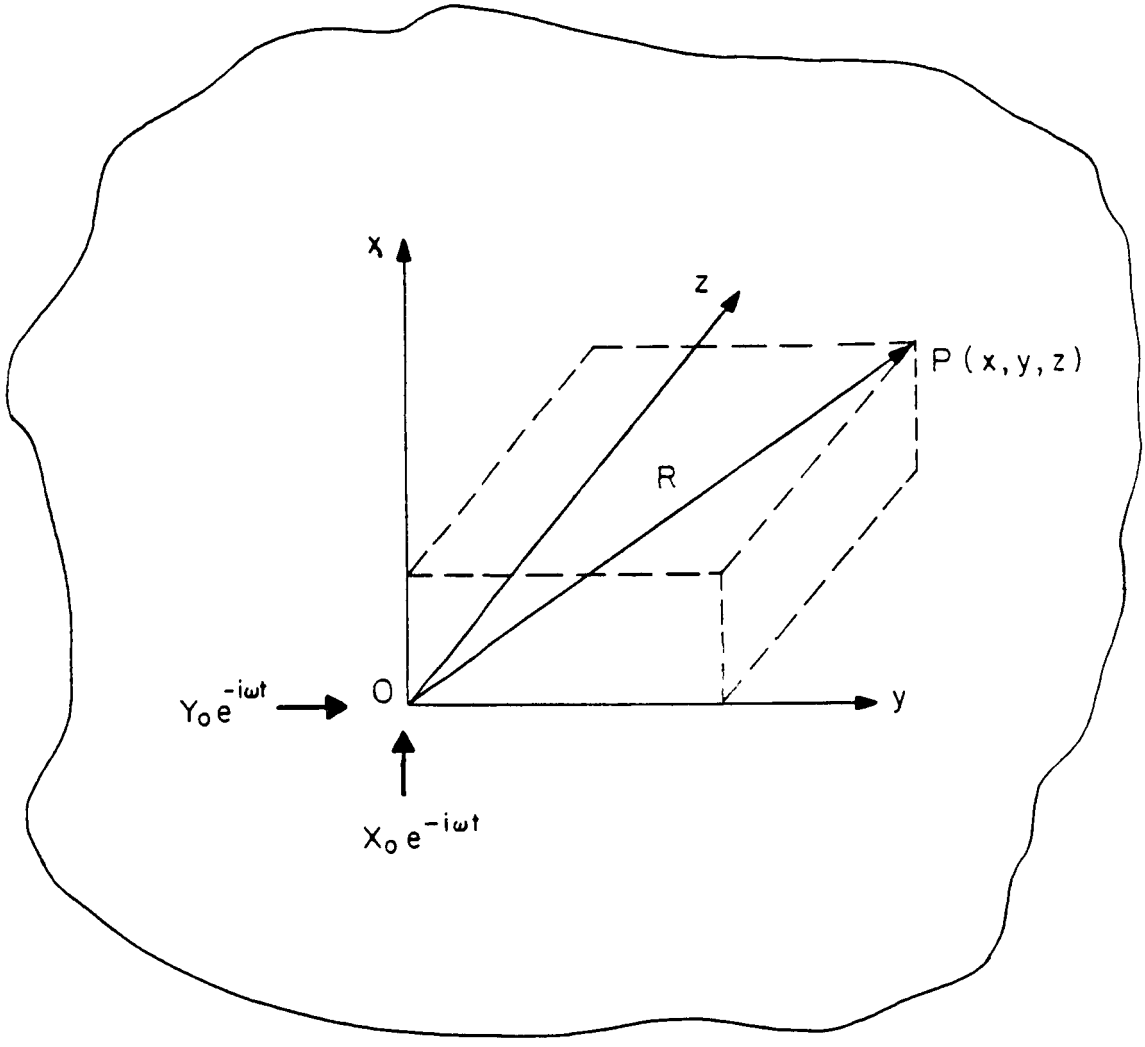

Fig. 9 Schematic illustrating harmonic point load exciting an infinite transversely isotropic medium, where xy is isotropic plane in cartesian coordinate system defined by (x,y,z).

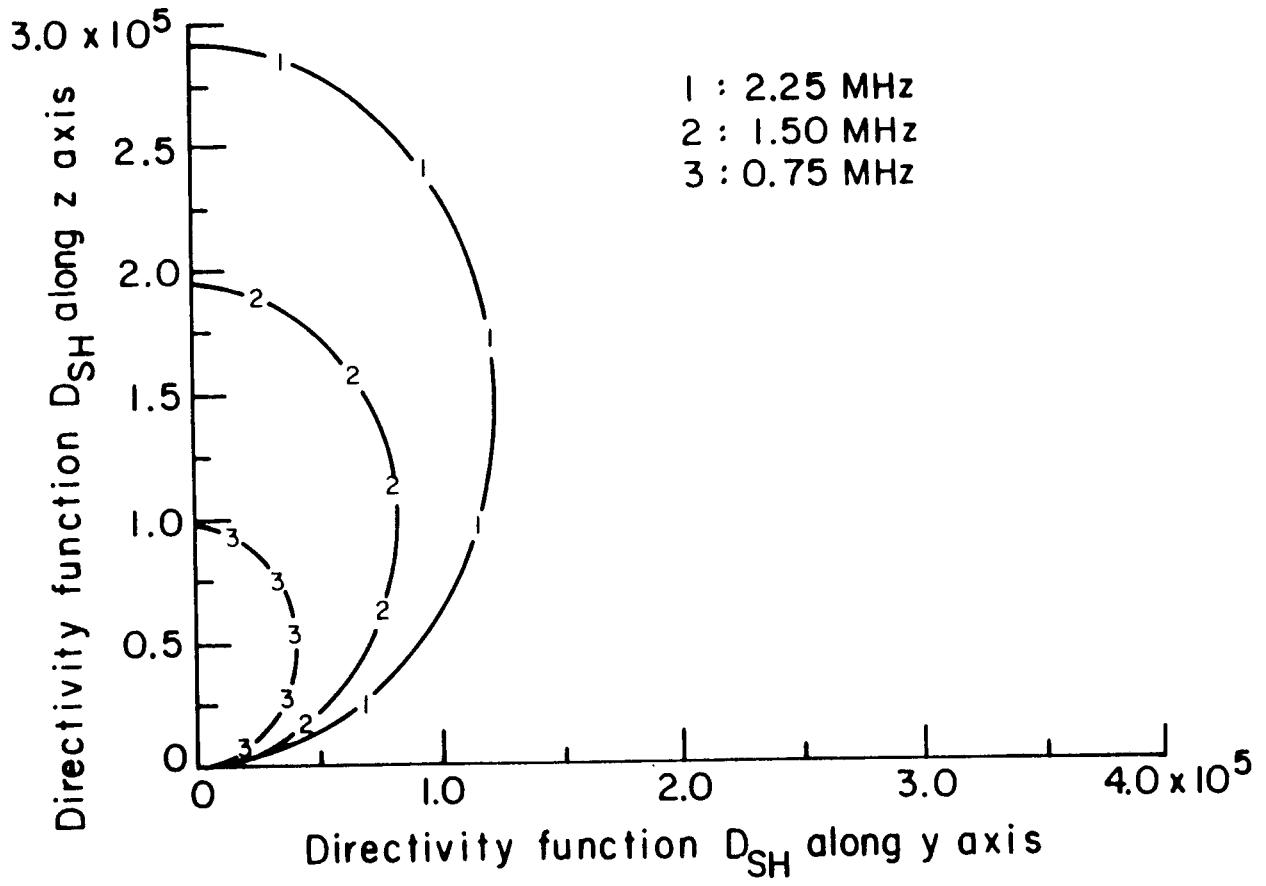

Fig. 10 Polar diagram of directivity function D_{SH} of shear stress τ_{xz} associated with SH waves at frequencies of 0.75, 1.50 and 2.25 MHz for positive y-z quadrant.

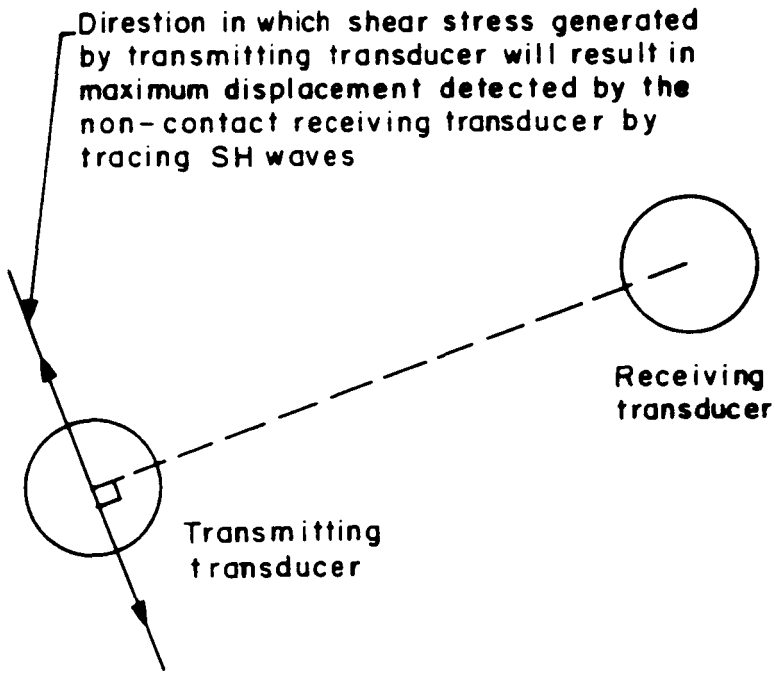

Fig. 11 Schematic illustrating maximization of displacement detected by non-contact receiving transducer by placing transmitting transducer such that shear stress generated by transmitting transducer is in direction perpendicular to line connecting transmitting and receiving transducers.

NASA
National Aeronautics and Space Administration

Report Documentation Page

1. Report No.	2. Government Accession No.	3. Recipient's Catalog No.
NASA CR-4087		

4. Title and Subtitle

Acousto-Ultrasonic Input-Output Characterization of Unidirectional Fiber Composite Plate by SH Waves

5. Report Date
August 1987

6. Performing Organization Code

7. Author(s)

James H. Williams, Jr., and Peter Liao

8. Performing Organization Report No.
None (E-3650)

10. Work Unit No.
506-43-11

9. Performing Organization Name and Address

Massachusetts Institute of Technology
Department of Mechanical Engineering
Cambridge, Massachusetts 02139

11. Contract or Grant No.
NAG3-328

13. Type of Report and Period Covered
Contractor Report
Final

12. Sponsoring Agency Name and Address

National Aeronautics and Space Administration
Lewis Research Center
Cleveland, Ohio 44135

14. Sponsoring Agency Code

15. Supplementary Notes

Project Manager, Alex Vary, Structures Division, NASA Lewis Research Center.

16. Abstract

A unidirectional fiberglass epoxy composite plate specimen is modelled as a homogeneous transversely isotropic continuum plate medium. Acousto-ultrasonic noncontact input-output characterization by tracing SH waves in the continuum is studied theoretically with a transmitting and a receiving transducer located on the same face of the plate. The single reflection problem at a stress-free plane boundary in a semi-infinite transversely isotropic medium whose isotropic plane is parallel to the plane boundary is analyzed first. It is found that an incident SH wave results in a reflected SH wave only; the amplitude ratio of the reflected SH wave to the incident SH wave is negative one; and the angle of reflection of the reflected SH wave is equal to the angle of incidence of the SH wave. The balance in energy flux normal to the plane boundary is also checked. The delay time is calculated as if the SH waves were propagating in an infinite half space. It is found that the directional dependence of the phase velocity of the SH waves travelling in the transversely isotropic medium has a significant effect on the delay time, as opposed to the directional independence of the phase velocity of the SH wave travelling in an isotropic medium. The displacement associated with the SH wave in the plate detected by the noncontact receiving transducer is approximated by an asymptotic solution for an infinite transversely isotropic medium subjected to a harmonic point load. The polar diagrams for the directivity function of the shear stress due to SH waves in the plate are shown at frequencies of 0.75, 1.50, and 2.25 MHz. To maximize signal detection, the transverse transmitting transducer should be placed such that the applied force generated by it is in the direction perpendicular to the line connecting the transmitting and the receiving transducers. This study enhances the quantitative understanding of acousto-ultrasonic nondestructive evaluation (NDE) parameters such as the stress wave factor (SWF) and wave propagation in fiber reinforced composites or any other materials which can be modelled as transversely isotropic media.

17. Key Words (Suggested by Author(s))	18. Distribution Statement
Ultrasonics; Acousto-ultrasonics; Nondestructive testing evaluation; Fiber composites; Stress waves; Stress wave factor	Unclassified - unlimited STAR Category 38

19. Security Classif. (of this report)	20. Security Classif. (of this page)	21. No of pages	22. Price*
Unclassified	Unclassified	48	A03

*For sale by the National Technical Information Service, Springfield, Virginia 22161

NASA-Langley, 1987